CONTROLLING THE WETTABILITY AND ADHESION OF CARBON FIBERS WITH POLYMER INTERFACES VIA GRAFTED NANOFIBERS

A Thesis

by

SEOKJIN HONG

Submitted to the Office of Graduate and Professional Studies of
Texas A&M University
in partial fulfillment of the requirements for the degree of

MASTER OF SCIENCE

Chair of Committee,	Mohammad Naraghi
Committee Members,	Ramesh Talreja
	Terry Creasy
Head of Department,	Ibrahim Karaman

December 2015

Major Subject: Materials Science and Engineering

ABSTRACT

Interfacial properties in carbon fiber composites is one of the key parameters controlling their structural functionality. Here, we introduce a novel method to engineering carbon fiber-epoxy interfaces, via inclusion of nanofibers, towards higher interfacial strength and energy dissipation. In our method, thermally stabilized polyacrylonitrile (PAN) nanofibers are grafted onto carbon fibers via electro-spinning process, followed by nanofiber consolidation via solvent vapor and thermal treatment. These treatments partially dissolve nanofibers along the nanofiber-fiber interface and trigger entropic elasticity in nanofibers thus, increasing the nanofiber-fiber interactions. The hybridization of carbon fibers with PAN nanofibers increased the interfacial shear strength (IFSS) by ~48%, from 10.8 ±2.6 to 15.9 ±4.9 MPa. Postmortem fractography points to mechanical interlocking between nanofibers and epoxy and reinforcing effects of nanofibers in matrix as root causes of IFSS enhancement. As a result of adding nanofibers to carbon fiber, junction failure mode changes from a dominantly adhesive failure (at epoxy-fiber interface) to dominantly cohesive failure, and failure plane slightly shifts away from epoxy-fiber interface to within the epoxy. Compared to other types of whiskers grown on carbon fibers, such as CNTs, the method proposed here requires low temperatures (below 300℃), during which no surface damages are expected to accumulate on carbon fibers.

ACKNOWLEDGEMENTS

I would first like to acknowledge my advisor, Dr. Mohammad Naraghi for his advice and support. Also, I would like to thank committee members, Dr. Ramesh Talreja, and Dr. Terry Creasy for their guidance and support throughout the course of this research.

Also, I thank my friends and colleagues in the research group and the department faculty and staff for making my time at Texas A&M University a great experience.

Finally, thanks to my parents and my younger brother for their encouragement, patience and love.

TABLE OF CONTENTS

LIST OF FIGURES

1. INTRODUCTION

1.1. Background and Literature Review

Carbon fibers are thin filaments largely (more than 90%) composed of carbon atoms with diameter ranging from 5 μm to 10 μm [1-3]. As promising materials for structural application and as the reinforcements in composite materials, the production and consumption of carbon fibers have steadily increased over the past few decades, and the growth is expected to continue in the next few decades [4].

The reason of the rising attention given to the carbon fibers is that they have remarkable mechanical properties at relatively low density, chemical corrosion resistance, high thermal stability, and good thermal and electrical conductivities [4-8]. For instance, the specific strength and modulus of carbon fibers is several times that of engineering materials, such as alloys, glass fibers and polymers (Figure 1). Due to these excellent properties, the carbon fibers have been used in various industries, such as aerospace, military, automobile sector and even sporting goods [4, 7, 9-11].

However, it is widely accepted that the mechanical properties of carbon fiber reinforced composites, such as in-plane and interlaminar strength, longitudinal and transverse strength and fracture toughness, are strongly and directly correlated with interfacial shear strength (IFSS) between the fiber and matrix [12-16].

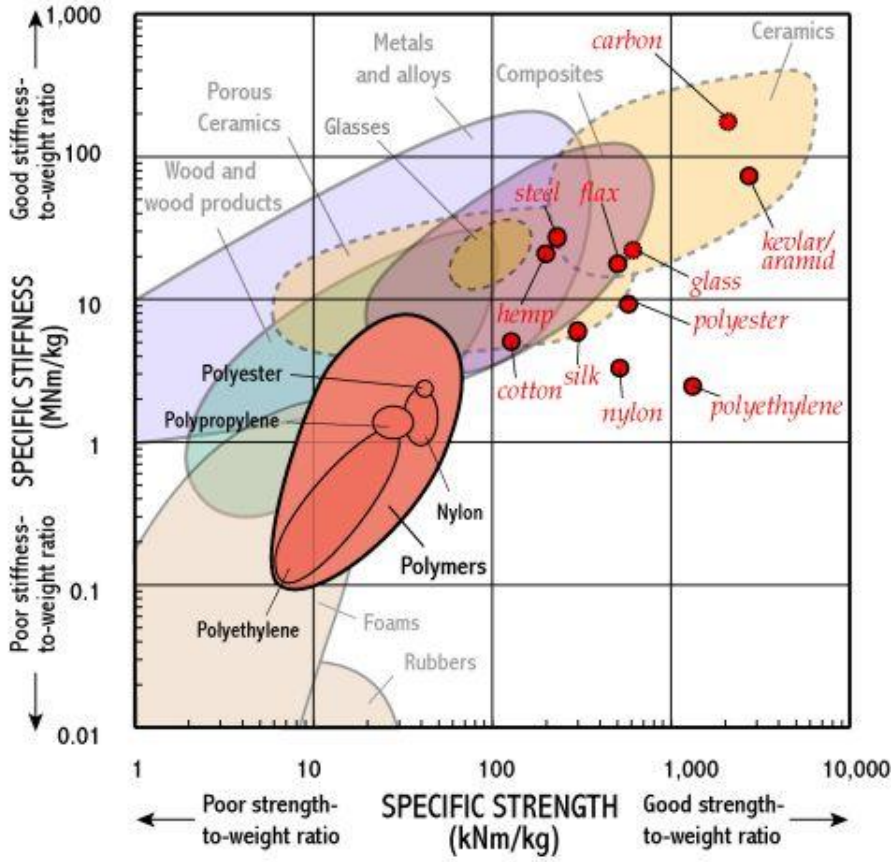

Figure 1. A comparison of strength and modulus of engineering materials. Carbon fibers appear on the top-right corner, with the high strength and modulus [Data taken from http://www-materials.eng.cam.ac.uk/mpsite/short/OCR/ropes/].

On the other hand, as-carbonized fibers typically have defective surfaces, which is due to high furnace temperatures experienced during carbonization (>800℃) [15, 17]. As a result of this high temperature, the as-fabricated carbon fibers are coated with atomically thin layers of polycyclic hydrocarbons [18]. The surface defects and hydrocarbons act as week bonding sites and lubricants between fiber and matrix, leading to poor fiber-matrix interactions, characterized by IFSS of as low as ~20–60 MPa [15, 17, 19-21].

To enhance fiber-matrix interactions, several approaches have been proposed and implemented, many of which have been extensively used in industrial scale. For example, a common practice in aerospace industry is oxidative treatment of carbon fiber surfaces, by which weakly bonded coatings are removed and fiber surfaces are chemically functionalized [22]. The functional groups will form chemical/physical bonds with epoxy matrices during the epoxy curing process, leading to improved IFSS [15, 17, 19, 20]. In addition, the oxidative treatment of the fiber surfaces can improve the surface roughness of the fiber, and lead to improvements in IFSS via mechanical interlocking [20]. Interestingly, through pull out experiments on surface functionalized carbon fibers where the intensity of chemical bonds with epoxy was controlled through further chemical treatments, Drzal *et al*. demonstrated that mechanical interlocking can have a significant contribution to interfacial shear strength between fiber and matrix, which is roughly equal to the contribution of chemical bonds.

Another approach to enhance fiber-matrix interactions is to grow or attach nanoscale whiskers with high aspect ratio and surface to volume ratio onto the surface of carbon fibers. The nanoscale whiskers substantially increase the load transfer area between the fibers and the matrix, leading to an enhancement in fiber-matrix interaction and effective IFSS [23, 24]. This approach is partly based on the inevitable increase in the surface of materials per unit volume/weight by reducing their characteristic length scale.

The composites reinforced with whiskerized (fuzzy) fibers may also be referred to as "hybrid composites", pointing to the hierarchy in length scale of reinforcements [25, 26]. Recently and in the past decade or so, the research on hybrid composites has taken a new turn by the introduction of carbon nanotube (CNT) and carbon nanofiber (CNF) coated carbon fibers. Several studies have investigated the chemical vapor deposition (CVD) of CNTs on carbon fibers, in which carbon fibers serve as the substrate [27-31]. These methods of CNT growth often require relatively high temperatures, above 600℃-900℃, which is often mandated by the requirements to grow CNTs regardless of the substrate.

Through single fiber pull out experiments, An *et al.* demonstrated that the CVD growth of CNTs on carbon fibers can improve IFSS by ~100%, from 65 MPa to 126 MPa. It was demonstrated that the CNTs served as anchors inside the matrix, improving the load transfer between the fiber and the matrix. The improvement in IFSS was partly a result of a dramatic increase in the load-transfer area between them [31]. Also, Sager et al. studied the effect of two different morphologies of CNTs grown by CVD, such as radially aligned and randomly oriented CNTs on carbon fibers, on the interfacial adhesion between carbon fibers and epoxy matrix. The radially aligned CNT and randomly oriented CNT coated carbon fibers demonstrated a 71% and 11% increase in interfacial shear strength over untreated carbon fiber. This increase may be because of the improved adhesion between carbon fiber and matrix and an increase in interphase shear yield strength due to the presence of carbon nanotubes [29].

However, as stated earlier, the CVD growth of CNTs on carbon fibers may lead to thermal degradation of the carbon fibers and catalyst diffusion inside carbon fibers, mainly due to high temperatures required for CNT growth, which will result in a considerable loss in mechanical strength of fibers [27, 29, 31]. The high temperatures will also remove the sizing, a proprietary polymer compound on the surface of carbon fibers, which serves as a protective layer to prevent carbon fiber wear and also to enhance carbon fiber wetting during resin infiltration.

To minimize carbon fiber thermal degradation, alternative recipes of CNT growth at temperatures as low as 500℃ have been carried out, with minimal damage to carbon fibers [32]. However, the CNTs formed at relatively low temperatures often are highly defective, and as such, the application of this method to improve IFSS is limited. To avoid fiber thermal degradation while maintaining high quality of CNTs, Garcia *et al*. transferred forests of CVF grown CNTs to prepreg carbon fibers at room temperature, which led to >100% increase in mode I and II fracture toughness [33].

An alternative method to develop hybrid fibers is electrophoresis (EP). This method allows for the deposition of a wide range of nanoscale reinforcements, such as CNTs, CNFs, and graphite nano-particles on carbon fibers [34-39]. Even through significant improvement in the fiber-matrix IFSS has been reported via this method, the exposure of the carbon fiber to an electric field in the electrophoresis solution led to damage in the fiber surface, which resulted in a 15–40% reduction in fiber strength depending on the

initial condition of the fiber, such as the surface chemistry of the fibers and the duration of electrophoresis [37].

Therefore, current whiskerization methods are faced with several challenges, such as carbon fiber degradation. In addition, in all the above methods, no clear path to enhance nanofiber-fiber interaction is presented. This is a major shortcoming, as poor fiber-nanofiber interaction will make the latter obsolete in terms of enhancing the interaction of the fiber with matrix. Moreover, the filler types are mainly limited to nanomaterials with high stiffness and strength (CNTs and CNFs), with no proposed method to extend them to more ductile nanomaterials such as polymeric nanofibers. The latter may be required to achieve strong and tough junctions in composites. Moreover, nanomaterials such as CNTs are often cost prohibitive for most composite applications.

To determine parameters of interfacial shear interaction between fiber and matrix, various micromechanical test methods have been developed. The test methods can be categorized into two groups. In one group, the external load is directly applied to fibers, while in another group of experiments, matrix is loaded via external means through which the interface is loaded [40-42]. The first group includes pull-out test, microbond test, and push-out test. In the pull-out test, uncured matrix is put onto a substrate of a plate shape and a fiber is vertically embedded into matrix. After curing the matrix, the fiber is pulled out of the matrix such that the interface is mainly loaded in shear [42]. In the microbond test, droplets of resin in micro-size are mounted on a fiber and each

mounted droplet forms around the fiber in the shape of ellipsoid. After the droplets on the fiber are cured, they are pulled out of the fiber to measure shear strength [41]. For the push-out test, specimens with a thickness of several hundred micro-scale are prepared. During the preparation of the specimens, fibers are embedded into a matrix in the thickness direction of the specimens. Then a diamond indenter is positioned on each fiber, and the fiber is pushed out of the matrix of the specimen by moving the indenter in vertical direction to evaluate interface parameters [40]. Another approach to load the interface is the single fiber fragmentation test in which the load is applied to the matrix via external means [43, 44]. For the fragmentation test, a specimen of dog-bone shape where a single fiber is embedded is prepared. Elongating the specimen in tension results in fiber breakage. With increasing level of strain, the number of fiber breakage gradually increases, ultimately leading to smaller fragments of fiber, where the length of fiber breakage is equal to the critical length. The fragmented length of the fiber cannot be further broken into smaller portions due to insufficient interfacial stresses, which cannot overcome the fiber strength. The interfacial shear strength is calculated by a force balance equation [43, 44]. The major limitation of the fragmentation test is the limited properties of the available matrix materials that are commonly employed. If the matrix materials is brittle, the matrix will break before the critical fragmented length of the fiber is reached. In the context, the microbond test can be one of the option for evaluation of interfacial strength because brittle matrix (epoxy) is used in our research. Therefore, we choose the microbond test and here we will call it single fiber pull-out test.

1.2. Objectives and Outline of Present Work

To overcome the aforementioned challenges in whiskerizing carbon fibers with nanomaterials as a means to enhance fiber-matrix interactions, we propose a new concept for hybrid composites, based on depositing thermally stable polymeric nanofibers on carbon fibers, in which the nanofiber-fiber interactions is controlled via exposure of nanofibers to vapor of the polymer solvent and temperatures below 300°C. This temperature is considerably below the thermal degradation of carbon fibers and sizing, thus, it prevents thermal degradation of carbon fibers. The polymeric nature of the nanofibers is expected to enhance the energy dissipation at the fiber-matrix interface, due to ductility of nanofibers [45], leading to strong and tough junctions.

In Section 2 we present the experimental methodology used to develop hybrid carbon fibers. The novel method used for fabricating a hybridized carbon fiber will be described in details. In addition, the mechanical and morphological characterization methods will be described. Section 3 begins with the morphological characterization of the new hybridized carbon fiber created by our novel method. The wettability of bare carbon fibers and hybridized carbon fibers will be compared to investigate the effect of nanofibers in enhancing the affinity of carbon fibers to matrix. In addition, the mechanical behavior of fiber-matrix junctions in pull-out test mode will be presented. Post-mortem images of the pull out surfaces will then be compared to identify the interface failure modes. Finally, in Section 4 we will summarize the conclusions of this study, and recommend future work on developing carbon fiber composites.

2. PROCESSING HYBRID CARBON FIBERS*

In this section, a new method to fabricate hybrid carbon fiber that are grafted with polymeric nanofibers is introduced. The nanofibers in this cases were polyacrylonitrile, with diameter ranging from about 50 nm to 300 nm. Our method to produce hybrid fibers includes 3 steps, electrospinning of nanofibers and attachment of nanofibers onto carbon fibers via solvent vapor and thermal treatments, followed by thermal stabilization of nanofibers. Through these step, hybrid carbon fiber have high roughness on their surfaces, with attachment of PAN nanofibers. The rough surfaces of the carbon fiber are observed by SEM images, and compared to those of carbon fibers. In addition, important factors which contributed to make the hybrid carbon fibers, especially the augmented entropic shrinkage of PAN nanofibers due to solvent and heat treatment and surface tension, is explained in details.

2.1. Materials

Single carbon fibers (SGP203CSDL), with average diameter of ~5.7 μm were purchased from Hexcel Corporation. Polyacrylonitrile (PAN) (MW=150,000) was purchased in powder form from Sigma-Aldrich. Dimethylformamide (DMF), purchased from Sigma-Aldrich, was used as the solvent to dissolve the PAN powder for nanofiber production via electrospinning process.

*Part of this section is reprinted with permission from "Controlling the Wettability and Adhesion of Carbon Fibers with Polymer Interfaces via Grafted Nanofibers" by Seokjin Hong, Majid Minary-Jolandan, and Mohammad Naraghi, 2015. *Composites Science and Technology*. **117**, 130-138, Copyright 2015 by Elsevier Limited.

2.2. Fabrication of Hybridized Carbon Fiber

Processing of hybridized carbon fibers was conducted in three steps, electrospinning a PAN solution onto a carbon fiber, exposing the electrospun PAN nanofibers grafted on the carbon fiber to DMF solvent, and thermally stabilizing the electrospun PAN nanofiber, as shown in Figure 2. In the first step, a single carbon fiber was fixed on to a copper frame, and the copper frame was placed and secured on the electrospinning drum collector. A PAN solution was made by mixing PAN powders of 2g with DMF solvent of 20.22g and stirring them at 80°C for 3 h to prepare a concentration of 9wt%. In addition, the air conditions in a chamber for electrospinning was made in relative humidity of 20% and at a temperature of 25℃. Then, the solution of PAN in a flow rate of 0.5ml/h was electrospun onto the single carbon fiber placed on the drum collector, under an applied voltage of 16kV, for 30 s. During the electrospinning, the distance between the tip of the syringe needle and the drum collector was 200mm. To ensure full coverage of the fiber surface, the solution of PAN was also electrospun onto the other side of the single carbon fiber for the same duration.

Scanning electron microscope (SEM) images of the grafted carbon fibers revealed that the majority of the nanofibers at this stage were laid parallel to the carbon fiber, and loosely attached to it (Figure 3). Such loosely attached nanofibers are not expected to transfer load between matrix and carbon fiber. Therefore, further processing steps were employed to enhance the fiber-matrix interactions. These steps were mainly guided by the following principle. It was argued that droplets of PAN solvent (DMF) placed on

fiber surface and then thermally evaporated can potentially enhance the contact area between PAN and carbon fiber partly by dissolving the nanofibers at their interface with carbon fibers. Moreover, evaporation of the liquid can induce surface tension, further pulling nanofibers towards the fiber. However, excessive solvent at the interface can completely dissolve the nanofibers.

Therefore, in step 2, to make the good adhesion between the carbon fiber and the electrospun PAN nanofibers, the saturated environment of DMF vapor was first set up by placing the DMF container on a hot plate at a temperature of 60℃ inside the chamber, as shown in Figure 2 (step2). Then the carbon fibers which were coated with electrospun PAN nanofibers were placed into the chamber to expose the electrospun PAN nanofiber to DMF vapor. It was intended to partially dissolve PAN at the nanofiber-fiber interface, thus increase the contact area and interactions between carbon fibers and the nanofibers.

Lastly (step 3), the PAN nanofibers electrospun on single carbon fibers were thermally stabilized in air, by exposing the carbon fiber to temperatures of as high as 265℃ for 2 h in an oven. During this process, several reactions take place in PAN nanofibers, including cyclization and de-hydrogenation, converting the molecular structure of the linear PAN into the ladder-like and more stable structure [46]. This step is critical in processing of hybrid fibers, since the as-fabricated PAN, unlike the stabilized PAN, will get dissolved in epoxy during the curing process (at temperatures of ~150–175 ℃). The steps are all shown in Figure 2.

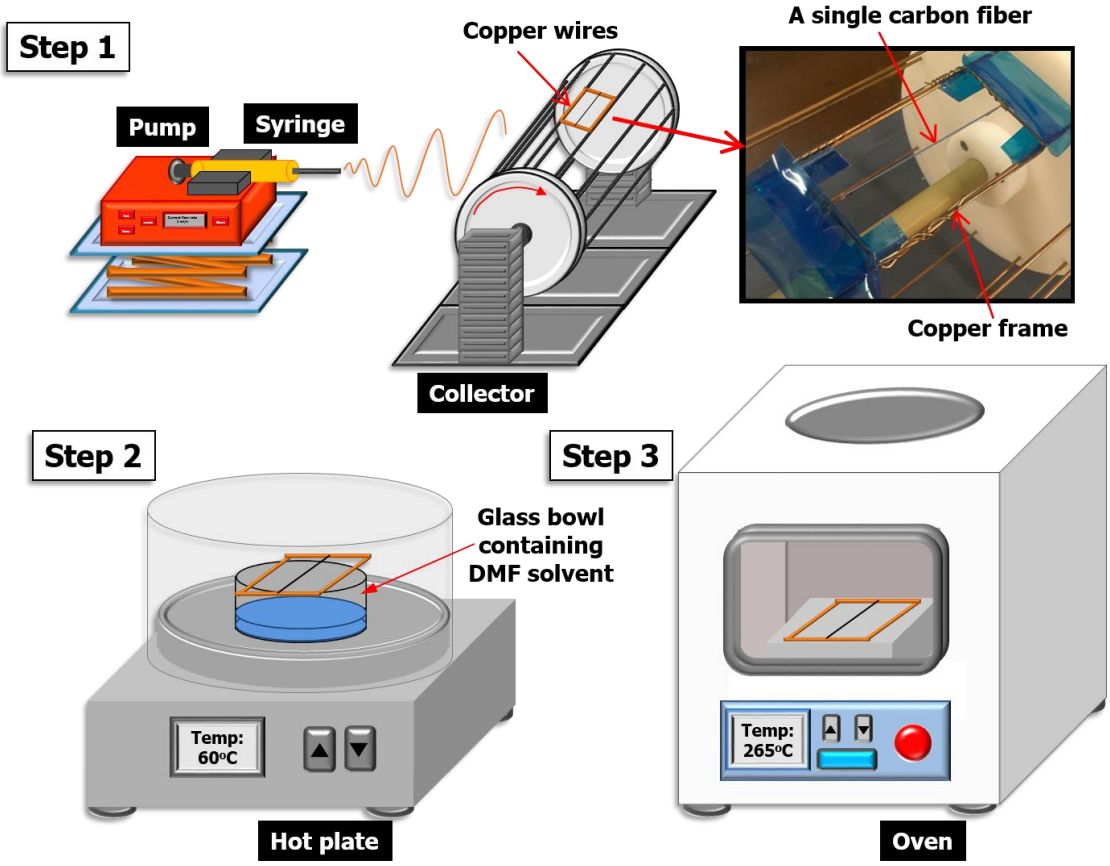

Figure 2. Schematics of steps for fabrication of hybridized carbon fibers: Step 1. Electrospinning nanofibers on single carbon fibers, Step 2. Exposure of a single carbon fiber which was grafted with electrospun PAN nanofibers to a vapor of DMF solvent, Step 3. Thermal stabilization of PAN nanofibers electrospun on the carbon fiber at 265℃.

2.3. Morphology of Carbon Fibers

The surface of carbon fibers, before and after nanofiber deposition, and before and after solvent vapor treatment were observed in Scanning Electron Microscope (SEM). SEM images of bare carbon fibers, and hybridized carbon fibers before and after solvent treatment, revealed the evolution of the fiber surface morphology during the hybridization process. As shown in Figure 3a, bare single carbon fibers have an average diameter of about 5.7 μm with smooth surfaces. In addition, as shown in Figure 3b, the as-electrospun nanofibers are mainly aligned with the axis of the fibers because of electrostatic attraction between the fibers and the nanofibers. On the other hand, it is evident in the figure that the majority of nanofibers are not directly connected to the carbon fiber. This arrangement of nanofibers is not likely to contribute to fiber matrix interactions due to poor fiber-nanofiber interactions.

As discussed in the previous section, to overcome this problem, the carbon fibers which were coated with PAN nanofibers were exposed to DMF vapor, as aforementioned in Fabrication of hybridized carbon fiber. The DMF vapor was intended to condense on surface of the carbon fiber and partially dissolve PAN nanofibers at the nanofiber-fiber interface, leading to increased contact area between the nanofibers and the fiber. The success of this approach in enhancing the interactions between nanofibers and the host fiber is evident, as nanofibers become conformal to the surfaces of fibers as a result of exposure to DMF (Figure 3c).

The hybridized fibers were then heat treated at 265℃ for 2 h to enhance thermal stability of PAN nanofibers in epoxy during the curing process, as discussed earlier. It is believed that part of the enhancement in fiber-nanofiber interface coverage is due to thermal treatment during which the solvent residues on the surface of carbon fiber is removed, In other words, as the menisci of solvent are evaporating, they generate a surface tension which pulls the nanofibers towards the fiber.

2.4. Mechanism Influencing Fiber-Nanofiber Interactions

It is evident from SEM images (Figure 3) that the contact area between nanofibers and carbon fibers increased drastically as a result of solvent vapor and heat treatment. There are two factors which contributed to the increased interaction between nanofibers and a carbon fiber during the solvent vapor treatment and thermal stabilization. First, as mentioned in Fabrication of hybridized carbon fiber, the DMF vapor condensates on carbon fiber surface, partially dissolving the PAN nanofibers near the fiber surface. The surface tension between DMF and PAN and also DMF and carbon fiber, as the DMF is being vaporized during PAN thermal stabilization, causes the nanofibers to collapse on the carbon fiber (Figure 4). As a result, nanofibers become conformal to fiber surface, and their contact is with carbon fiber increased (schematically shown in Figure 4).

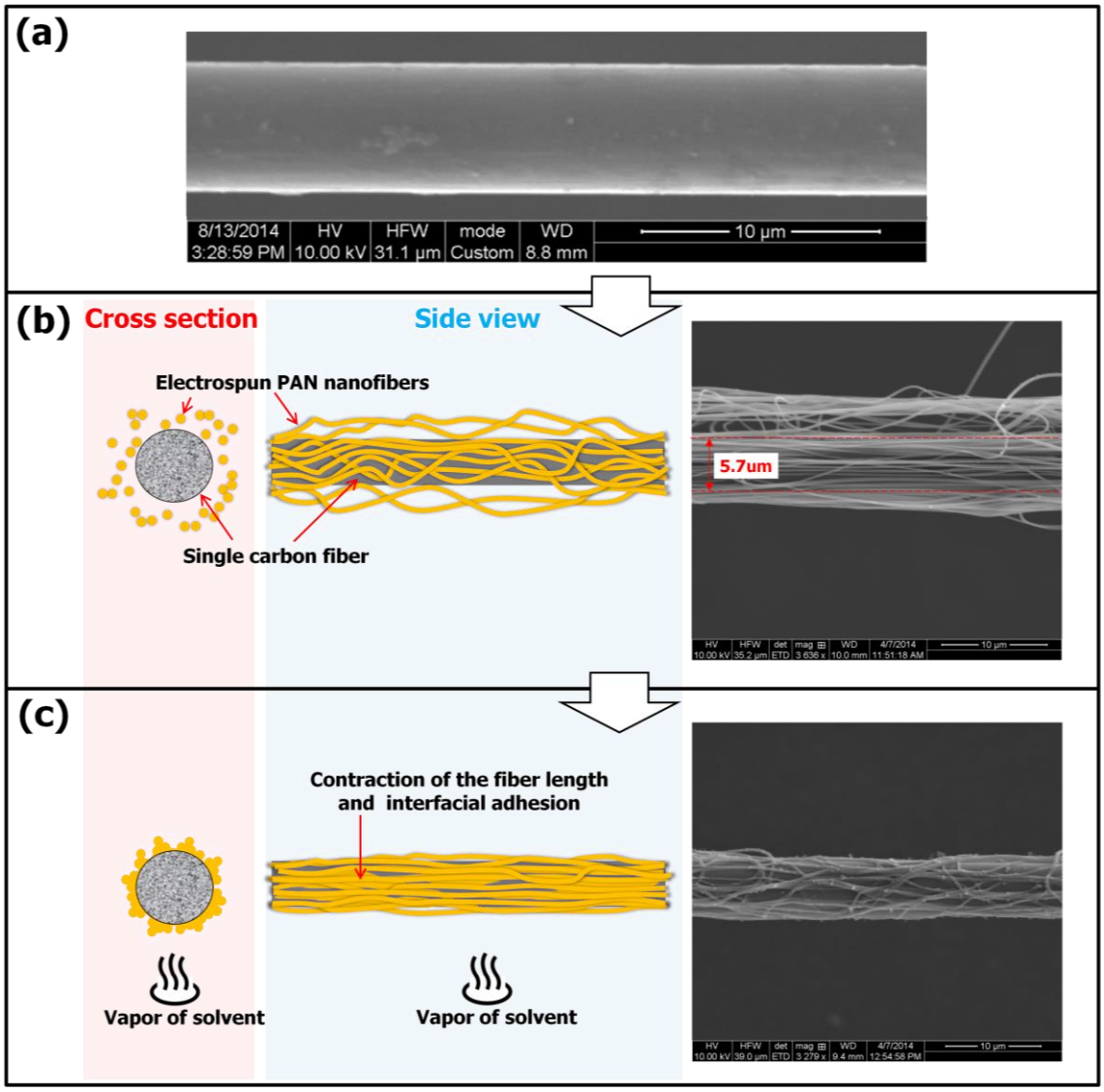

Figure 3. Schematic illustration and corresponding SEM images of the formation of hybridized carbon fibers. (a) Bare carbon fiber. (b) Carbon fibers coated with as-electrospun nanofibers. (c) Hybridized carbon fibers after solvent vapor treatment and thermal stabilization.

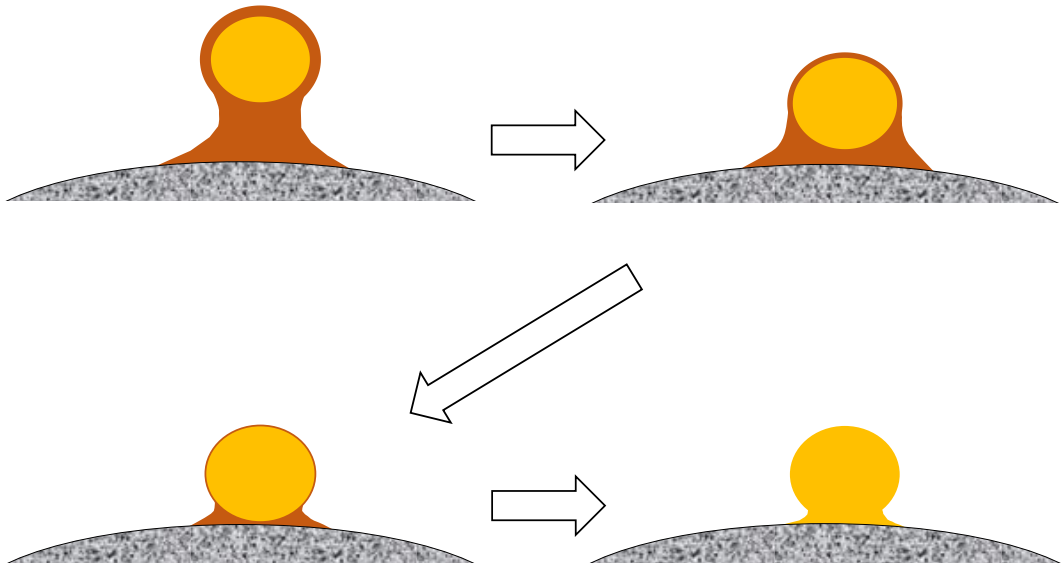

Figure 4. Schematic illustration of conformation of nanofibers to carbon fiber surface: solvent evaporation and surface tension contribute to the conformation.

The second cause is rooted in the molecular alignment and crystallinity of electrospun PAN nanofibers [47]. In other words, as electrospun PAN nanofbers contain chains that are partially aligned with nanofiber axis, caused by electrostatic stretching during electrospinning process. Due to chain alignment and order in chain arrangement, the entropy of the as electrospun PAN nanofibers is less than a maximum which can be achieved in the case of random alignment (Figure 5). This chain alignment is stable at room temperature due to low solvent content of the as electrospun nanofibers [47]. However, the diffusion of DMF to PAN nanofibers (step 2 in Figure 2) which had been deposited on carbon fibers acts as a plasticizer in PAN and increases the chain mobility [48, 49]. The chain mobility will be further enhanced during thermal stabilization (step 3 in Figure 2), as the temperature of PAN is raised above its Tg (~90℃). The enhanced chain mobility will inherently relax the aligned chains and deform the fiber towards maximum entropy. Hence, chains retract and the nanofibers length will shrink. As a result, the PAN nanofibers which are partly conformal to fiber surface due to DMF surface tension will tightly wrap around the carbon fiber, further enhancing fiber-nanofiber interaction (Figure 5).

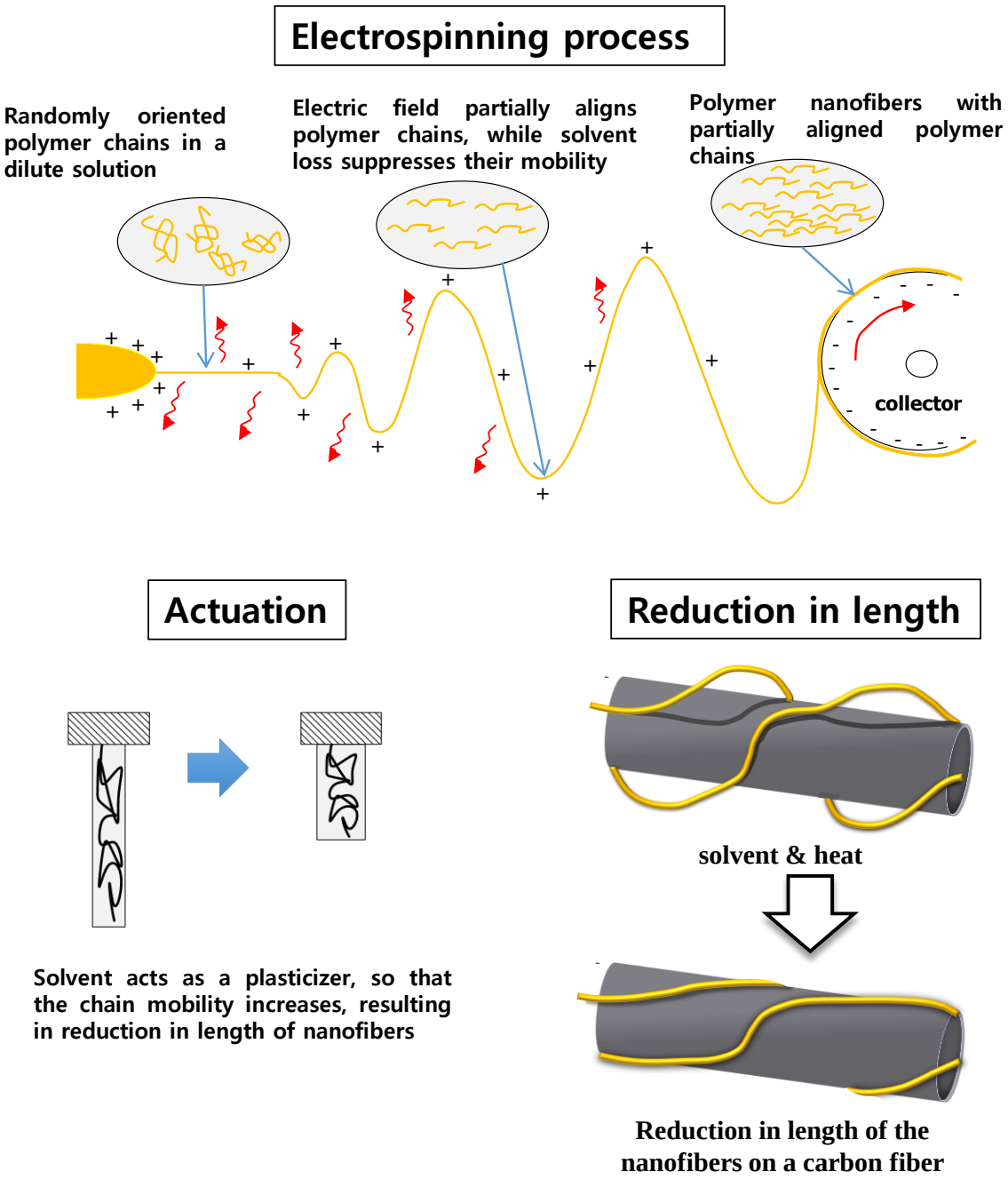

Figure 5. Schematic illustration of chain alignment and reduction in length of nanofibers; top figure: polymer chains are aligned via electrospinning process due to electric force and mechanical force, left figure: the mobility of the aligned chains is activated by solvent, right figure: nanofibers are conformal to the carbon fiber surface due to reduction in length of the nanofibers induced by solvent and heat

To study the magnitude of this length change, we exposed free standing electrospun ribbons of PAN to saturated environment of DMF solvent followed by thermal stabilization, and monitored their length change. The steps were similar to those applied to PAN nanofiber coatings of hybridized carbon fibers, as shown in Figure 2. The optical images of the PAN ribbon before and after solvent treatment and thermal stabilization are shown in Figure 6a, pointing to a considerable change in length after each of the two steps. As shown in Figure 6b, the length of the ribbon of nanofibers reduced by ~20% after solvent vapor treatment, and the total change in length nearly tripled after thermal stabilization. The change in length is calculated relative to the final length of the ribbons as the reference length. This change in length, for the nanofibers that are conformal to the fiber surface (for instance via surface tension), will tighten the nanofibers around the carbon fiber, leading to enhanced friction and load transfer between them.

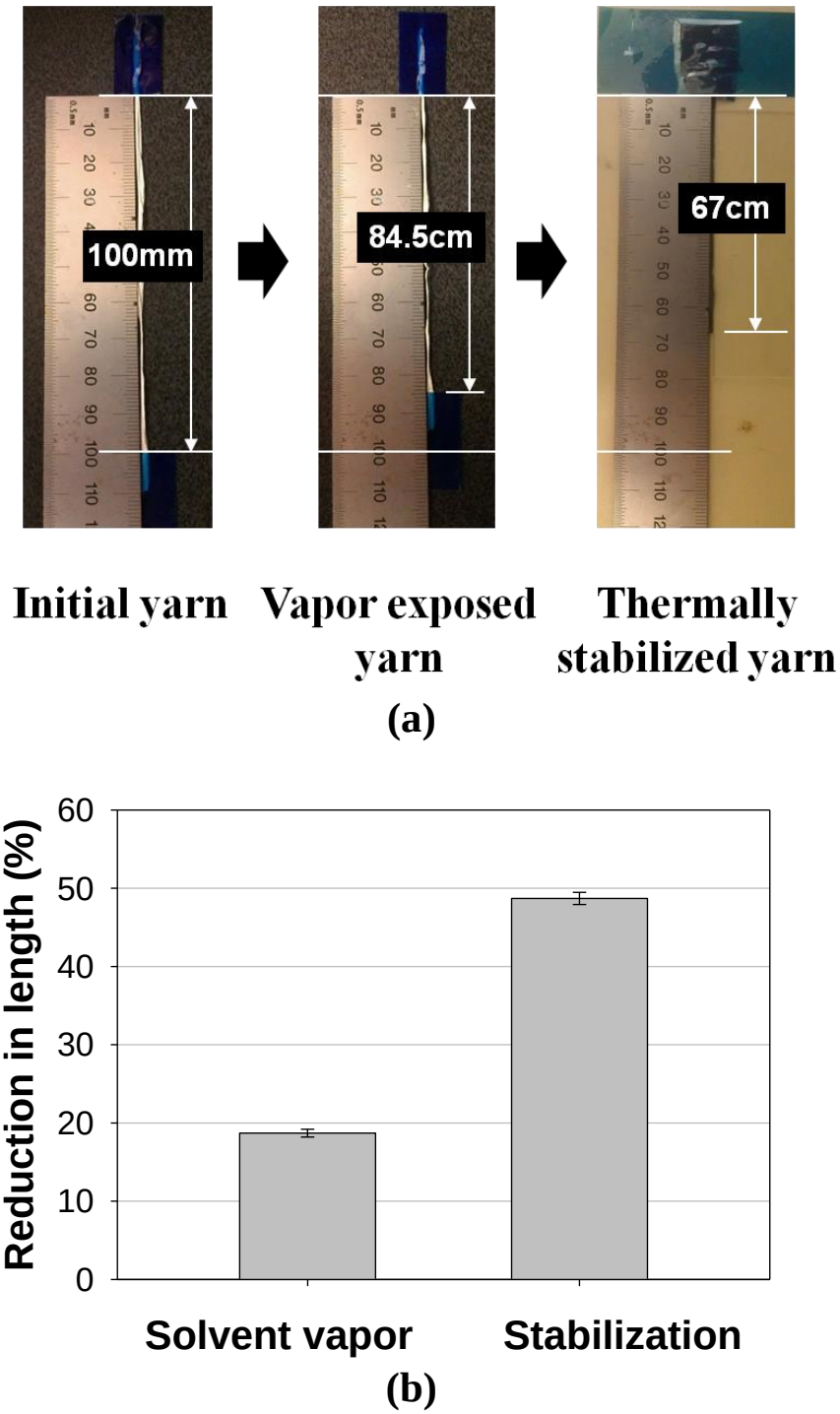

Figure 6. (a) Entropy driven shrinkage of electrospun PAN nanofiber yarns induced by solvent vapor and heat during stabilization. (b) Reduction in length normalized by the final length.

2.5. Conclusion

The hybridized carbon fibers were well fabricated by using three steps, electrospinning technique, vapor condensation, and thermal stabilization. For the first step, a carbon fiber was fixed on a copper frame, and the copper frame was placed on a collector, and then a prepared PAN solution was electrospun onto the carbon fiber. It was observed that the electrospun nanofibers was loosely aligned along the carbon fiber indicating that a load applied cannot be transferred from matrix to the carbon fiber due to the incomplete adhesion between the carbon fiber and the nanofibers. The poor adhesion was very well improved by exposing the nanofibers to DMF vapor in a chamber. That is partly because the surface tension between DMF and PAN as well as DMF and carbon fiber pulled the nanofibers to the carbon fiber. Moreover, the PAN nanofibers were partly dissolved at their interface of carbon fiber, thus, the contact area between carbon fiber and nanofibers increased. Moreover, the diffused DMF solution into PAN nanofiber acted as plasticizer, thus, enhancing polymer chain mobility. As a result, the length of nanofibers was shrunk and they wrapped tightly around carbon fibers. After the solvent vapor treatment, the PAN nanofibers grafted on carbon fiber were thermally stabilized to make sure that the nanofiber are thermally stable and they will not dissolved in the epoxy during the curing process. The well-made hybridized carbon fibers were expected to have good adhesion to epoxy matrix based on the increased high surface roughness of carbon fiber, as discussed in the following section.

3. AFFINITY OF CARBON FIBER-EPOXY CAUSED BY FIBER HYBRIDIZATION*

In this section, two methods to evaluate the affinity of carbon fibers to epoxy as a result of hybridization of the fiber with nanofibers is incorporated. The first method is intended to indicate the wettability of carbon fibers by the epoxy matrix by measuring the contact angles between carbon fiber and epoxy matrix. Based on contact angle measurement, we found that hybridized carbon fiber shows better wettability with smaller contact angle compared to carbon fiber, which may imply an affinity between stabilized PAN nanofibers and carbon fiber. The higher contact angle of hybridized fibers is explained in terms of their higher surface roughness relative to bare fiber and physical interactions between nanofibers and matrix. The second method is to evaluate the interfacial shear strength (IFSS) between fiber and matrix through pulling out carbon fibers from epoxy microdroplets. From the results, it is revealed that the nanofibers grafted onto carbon fiber can change the failure mode from a brittle-like to ductile failure, as evident from the added roughness of the fracture surface, an indication of higher adhesion and energy dissipation. Also, the surface morphologies of the carbon fibers and the internal surface of the hole of microdroplets are observed with the postmortem SEM images. While the carbon fiber surface mostly has adhesive failures indicating weak adhesion, the hybridized carbon fiber surface mainly represents

*Part of this section is reprinted with permission from "Controlling the Wettability and Adhesion of Carbon Fibers with Polymer Interfaces via Grafted Nanofibers" by Seokjin Hong, Majid Minary-Jolandan, and Mohammad Naraghi, 2015. *Composites Science and Technology*. **117**, 130-138, Copyright 2015 by Elsevier Limited.

cohesive failures with rough surfaces, which also corresponds to the internal surface of the hole of the microdroplet pulled out. The rough surface with grooves represents the increased failure surface which indicates more energy dissipation. Ultimately, the failure mechanism is proposed in the last discussion based on the observation.

3.1. Materials

Inspired by the wide-spread use of epoxy matrix in aerospace engineering, the matrix used in the experiments was EPON 826 and its curing agent was EPIKURE W. Epoxy resin and curing agent, (EPON 826 and EPIKURE W, respectively), were purchased from Miller-Stephenson Chemical Company, Inc., and were used to make epoxy micro-droplets on carbon fibers and hybridized carbon fibers.

3.2. Surface Wettability Measurement of Carbon Fibers

The contact angle of the epoxy microdroplets embedded with bare and hybridized carbon fiber was measured via optical microscopy as shown in Figure 7. The hybridized carbon fiber/epoxy microdroplet composite has a markedly lower contact angle compared to bare carbon fiber/epoxy micro-droplet composite (56.6° compared to 73.4°), indicating a higher wettability between hybridized carbon fiber and the matrix. The higher wettability of hybridized fibers suggests an affinity between stabilized PAN and epoxy (Figure 7). Moreover, the increased surface roughness of the hybridized carbon fibers compared to bare fibers is partly responsible for the enhanced wettability of the former, as the interface between liquid epoxy (prior to curing) will follow the rougher

surface of hybridized fibers to minimize the surface energy. In other words, it can be argued that on the surface of hybridized carbon fibers, small pockets of epoxy wet the carbon fiber which are surrounded by nanofibers on the surface of carbon fibers. The contact angle of the rest of the epoxy droplet with this surface layer by definition is zero (epoxy-epoxy interface). However, at other areas on the carbon fiber, the epoxy droplet is in contact with the nanofibers or carbon fiber with higher contact angle. Therefore, the macroscopic contact angle will get some value in between zero (contact angle of the epoxy-epoxy interface) and a finite value which can be as high as the contact angle of epoxy to bare carbon fiber (Figure 8).

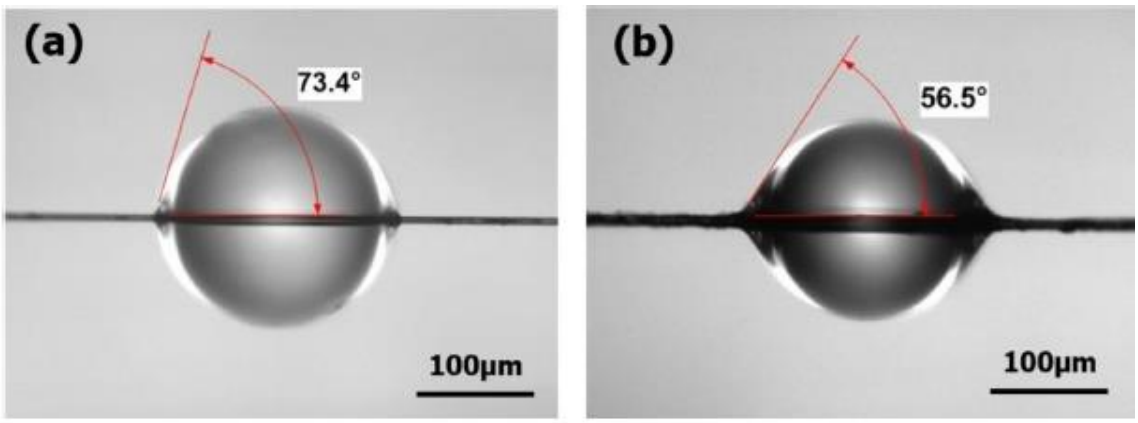

Figure 7. Contact angles between epoxy with (a) bare and (b) hybridized carbon fiber.

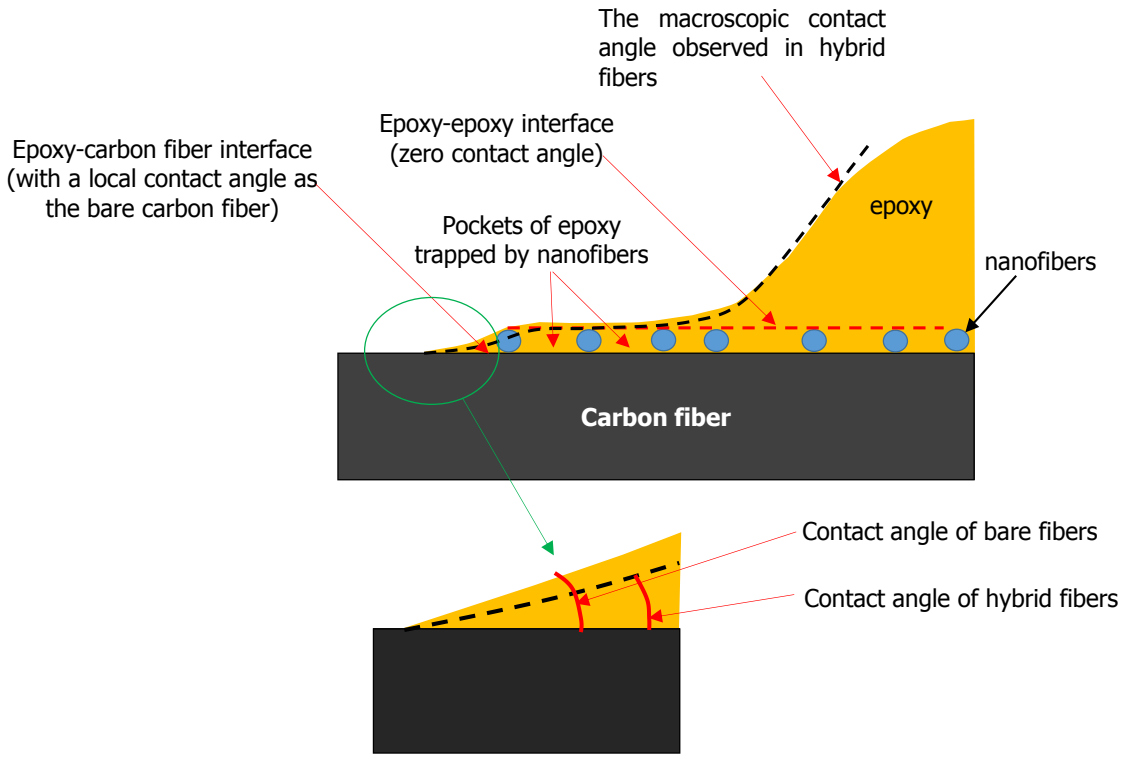

Figure 8. The mechanism of wettability induced by surface roughness.

3.3. Single Fiber Pull-out Test

To evaluate the IFSS of carbon fibers and Epon 862 epoxy, single fiber pull out tests from cured epoxy droplets were carried out. To this end, epoxy micro-droplets were placed on single bare and hybrid carbon fibers. The epoxy was made by mixing resin/curing agent with a weight ratio of 1 to 0.264. The droplets, in liquid form and prior to curing, were placed on fibers by using a needle with a fine tip. The epoxy micro-droplets were cured for 2 h at 125℃ and then for 2 h at 175℃ inside an oven. The

diameter of the epoxy microdroplets ranged from about 45 μm to about 258 μm, fairly controllable based on the initial (prior to curing) size of the droplet. Larger droplet sizes were not suitable for IFSS measurements, simply because they led to fiber rupture instead of fiber pull out, since the interfacial forces were more than the strength of the fiber. Moreover, smaller droplets were avoided due to experimental limitations, including the relatively low magnitude of pull out force they can bear comparable to force measurement resolution and difficulties in mounting smaller droplet sizes on fibers. Examples of carbon fibers, partially embedded in cured epoxy droplets, are shown in Figure 10a and b.

The pull out tests were performed on a Gatan MT10365 tensile testing device with modified grip. The grip was designed as shown in Figure 10a, then it was fixed on the Gatan tensile tester as shown in Figure 10b.

To perform the pull out tests, the carbon fiber with the epoxy droplet was placed on the device, with its one end fixed to the load cell, while the epoxy micro-droplets were carefully placed across a channel with the width of ~20 μm. This width was sufficiently wider than the fiber diameter and narrower than the diameter of the droplet to allow for friction free sliding of the fiber while blocking the motion of the droplet when the device is actuated, thus loading the fiber-matrix interface in shear (Figure 10b).

The single fiber pull-out tests were carried out with a cross-head speed of 2 μm/min. The average value of the interfacial shear strength (IFSS) τ_{IFSS} was estimated as:

$$\tau_{IFSS} = \frac{F_{max}}{\pi \cdot d \cdot l} \quad (1)$$

where F_{max}, d, and l are the junction load capacity (the maximum load on the fiber and the junction at which the failure was initiated), diameter of single carbon fibers and the embedded length of the fibers in epoxy droplet, respectively. A minimum of 13 experiments were performed for each type of fibers (bare or hybridized).

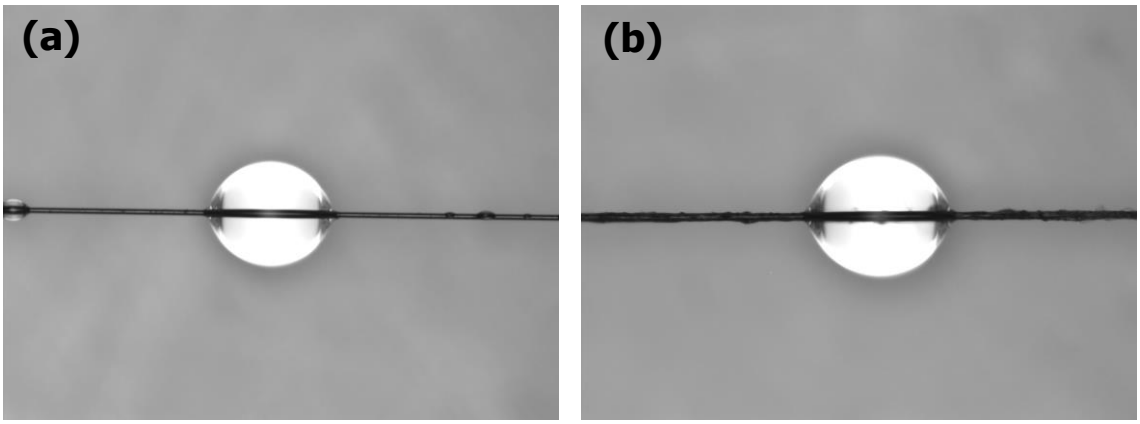

Figure 9. Optical microscope images of (a) an epoxy micro-droplet on a bare and (b) hybridized carbon fiber.

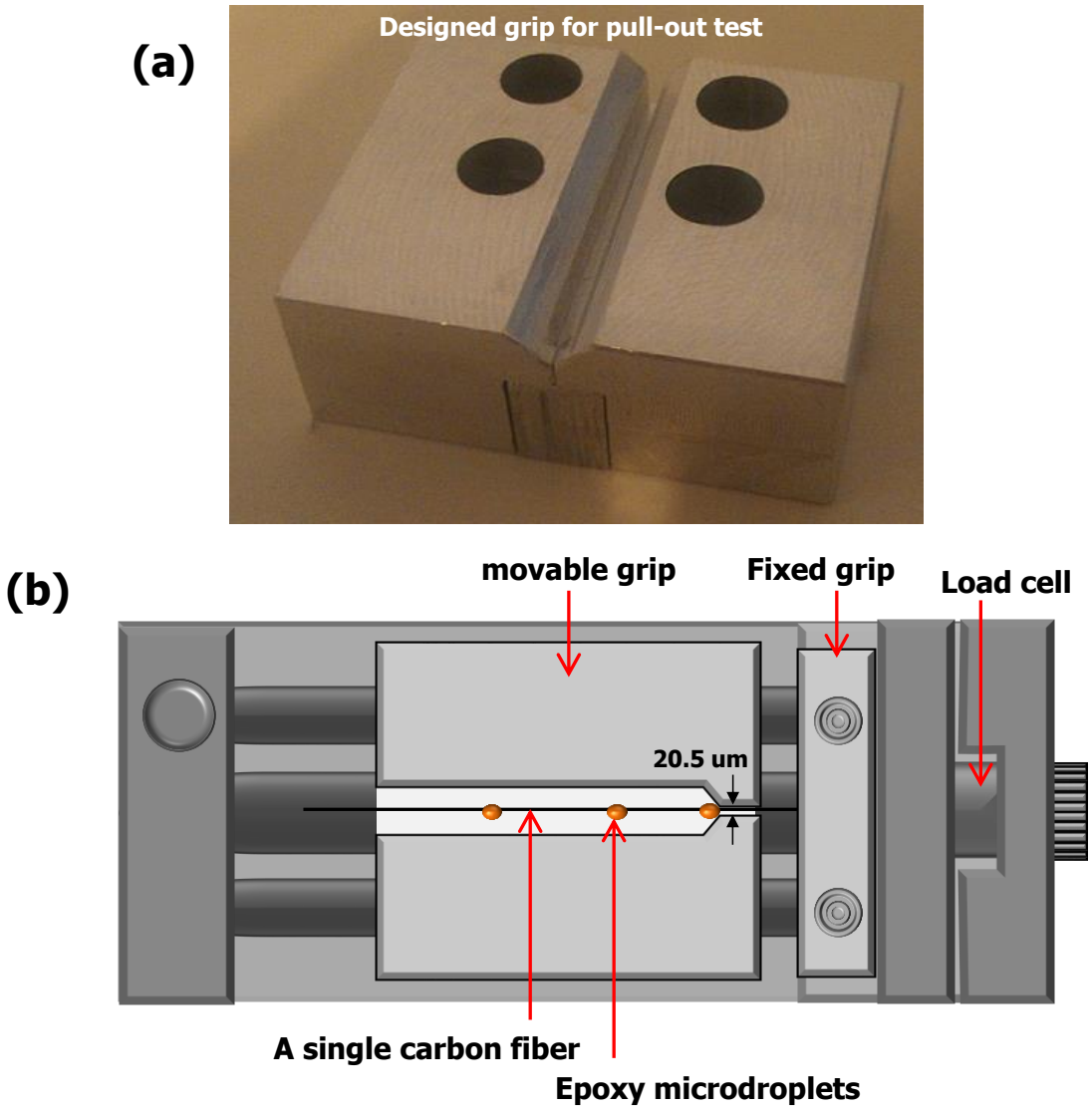

Figure 10. Device for pull out test: (a) Grip designed. (b) Schematic of the modified tensile tester machine to perform the pull out experiment.

3.4. The Results of Single Fiber Pull-Out Test

Pull-out experiments were carried out to evaluate the effect of carbon fiber hybridization on interfacial shear strength between fiber and epoxy matrix. During each pull out test, the force applied on the junction was increased until the junction failed. The maximum force on the fiber, which is equal to the total force carried by the fiber-matrix interface (due to force equilibrium of carbon fiber), was recorded as a function of the cross head displacement.

An example of the force *vs*. cross head displacement for the two cases of bare and hybridized carbon fibers is shown in Figure 11a and b, respectively. As shown in the Figure 11, the force initially increases linearly in both types of fibers, until the force capacity of the junction is reached and the junction fails. However, the post-peak mechanical behavior of the junctions is markedly different between the two types of fibers. In the case of bare fibers, the junction failure was catastrophic, and subsequent to reaching the peak force, the junction lost nearly its entire load bearing capacity. In contrast, in hybrid fibers, the junction failure was not catastrophic. Instead, subsequent to reaching the peak load, junction retained a considerable portion of its load bearing capacity, with significant energy being dissipated in the post-peak sliding. More interestingly, in a few hybrid fibers, a second force peak, higher than the first peak was observed. This post-peak residual load capacity is caused by mechanical interlocking at the interface of nanofiber coated fibers and epoxy droplet. Therefore, our proposed approach for carbon fiber hybridization offers great potential to enhance both junction

strength (load bearing capacity) and toughness (post-peak energy dissipation). However, it is to be pointed out that more research is needed here to characterize the post-peak behavior, as this residual load capacity showed a considerable scatter between different samples, likely due to variations in surface roughness of hybridized carbon fibers along their length.

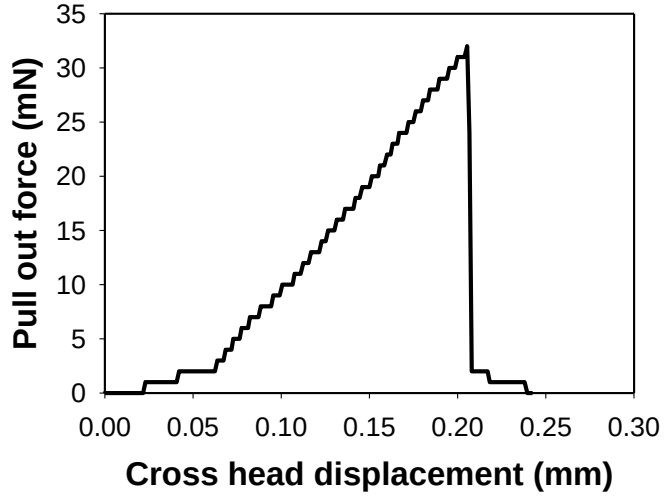

(a)

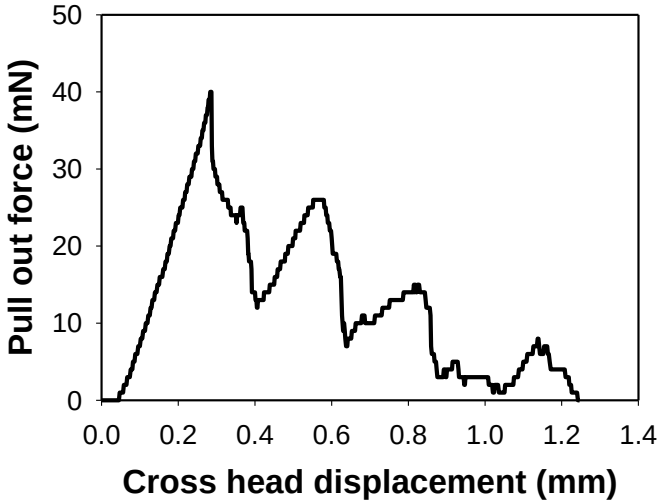

(b)

Figure 11. Pull out force *vs.* cross-head displacement curves of (a) bare and (b) hybridized carbon fibers from epoxy microdroplets.

To investigate the effect of carbon fiber hybridization on load bearing capacity of junctions, the pull out tests were interpreted in terms of effective IFSS, calculated based on Equation (1). As shown in Figure 12, hybridization of carbon fibers with thermally stabilized PAN nanofibers increased the IFSS on average by ~48%, from 10.8 ± 2.6 MPa to 15.9 ± 4.9 MPa. The uncertainties in the measurements are the standard deviations of a minimum of 13 measurements. Higher uncertainty in the IFSS of hybridized fibers is potentially rooted in non-uniformities in the nanofiber coatings between samples and/or along each sample.

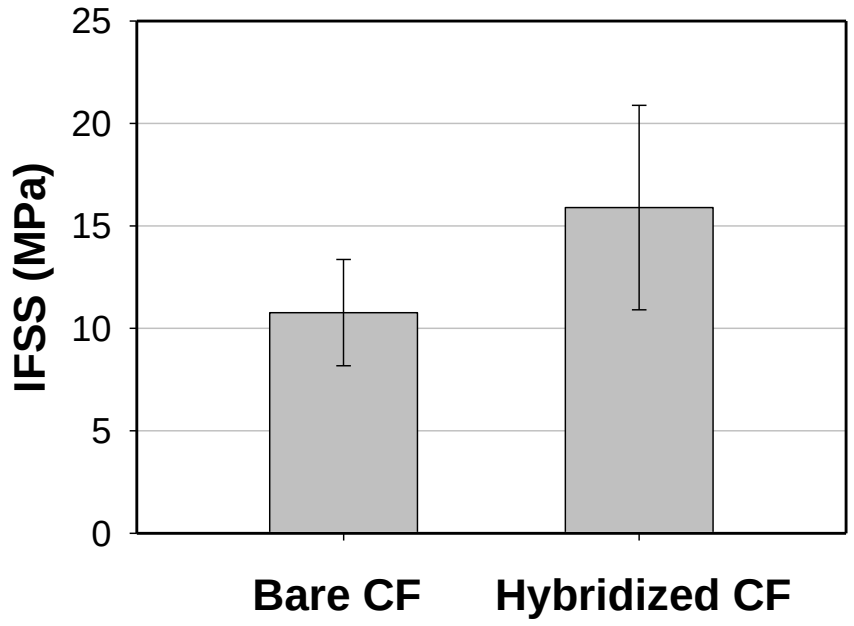

Figure 12. Comparison of IFSS of bare and hybridized carbon fiber/epoxy micro-droplet.

3.5. Effect of Exposure of Fibers to DMF and Heat Treatment

In addition to comparisons made between IFSS of hybridized carbon fibers and as-received bare fibers, to investigate the possibility of sizing removal and accumulation of surface damages on carbon fibers as a result of DMF vapor and heat treatments, we exposed a few bare carbon fibers to 265℃ and DMF vapor, following the protocol that was used to coat carbon fibers with PAN nanofibers. The treated bare carbon fibers revealed an IFSS of 9.9 ± 2.2 MPa and wetting angle of 70.2° with the epoxy, very close to the corresponding values of the as-received (untreated) bare carbon fibers, 10.8 ± 2.6 MPa and 73.4°, respectively. Hence, the adhesion and interactions between the epoxy and the carbon fibers – in the absence of nanofibers – is not influenced by our proposed treatments. As such, it is concluded that surface of the carbon fiber remains unchanged, ruling out the possibility of sizing removal. Moreover, since the sizing removal is the prelude to the accumulation of damage on carbon fibers, the possibility of the latter is also excluded.

3.6. Fractography and Interfacial Failure Mechanism

More insight into the origin of IFSS enhancement via nanofiber hybridization was obtained by postmortem SEM imaging of pulled out fibers and their epoxy holes. Typical images of fibers and holes for both bare and hybridized fibers are shown side by side in Figure 13. Postmortem images of bare carbon fibers points to a dominantly adhesive junction failure, along the fiber-matrix interface, evident from the clean surfaces of the pulled out fibers (no or insignificant epoxy residues). For instance, the

portions of the fiber shown with rectangles (1) and (2) in Figure 13a, and their zoomed in views in Figure 13b point to a dominantly clean fiber surface after pull out (rupture along the fiber-epoxy interface). The boundaries of the epoxy droplet prior to pull out are shown with broken lines in Figure 13a for clarity. It is to be noted that cohesive failure (within the matrix) of the bare fiber-epoxy junction along a surface parallel to the fiber surface was also observed with lower frequency than adhesive failure, as it is evident from the epoxy residues in some portions of the fiber, *e.g.*, shown in Figure 13b.

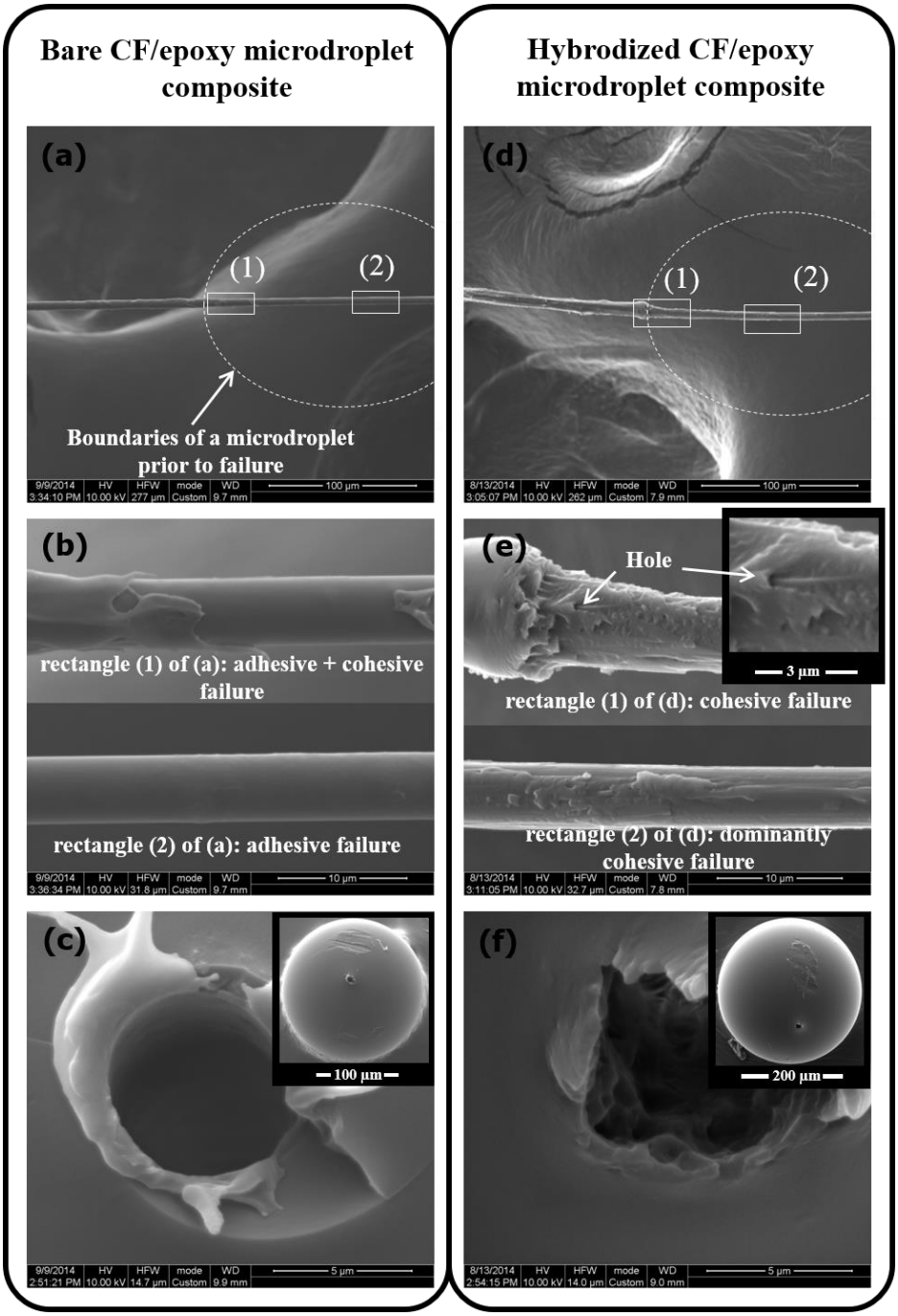

Figure 13. Postmortem SEM images of surface morphology of (a & b) bare and (d & e) hybridized carbon fiber. In (a) and (d), the boundaries of epoxy microdroplets prior to failure is shown with broken lines. The inner surface morphologies of the micro-droplet holes for the two cases of (c) bare and (f) hybridized fibers. The insets in (c) and (f) are SEM images of pulled out droplets. The pull out hole can be discerned in the inset.

In contrast to bare fibers, post failure SEM images of the hybridized fibers, along the initial embedded length, suggests that their junction failure is mostly cohesive. The epoxy residues on the pulled out fibers, shown in Figure 13d and e, are indications of cohesive failure of the junction within the epoxy near the fiber-epoxy interface. Rare cases of adhesive failure were also observed, such as the portions of the fiber with no apparent epoxy residue in rectangle 2 of Figure 13d and the zoomed out view in Figure 13e. These cases have likely occurred at locations where the local density of the PAN nanofibers was low, as this type of failure is similar to dominant failure mode of bare fibers. In addition, the diameter of epoxy holes for the case of bare fiber pull out is close to the fiber diameter, while for hybridized fibers, the holes are slightly larger than the diameter of the bare fibers, consistent with the adhesive and cohesive junction failures of bare and hybridized fibers, respectively.

Moreover, a comparison between the surface morphology of the epoxy holes for the two cases of fibers reveals that the postmortem surfaces of the holes have a considerably higher roughness in case of hybridized fibers compared to bare ones (compare Figure 13c and f). The rough surfaces of the former can be explained based on mechanical interactions between the epoxy and PAN nanofibers, such as reinforcing effect of the latter, which prevented the propagation of the interfacial debonding along the fiber-matrix interface, consistent with the predominantly cohesive junction failure of epoxy-hybridized fibers (Figure 13e).

Assuming that the cohesive failure leading to pull out is stress-driven, higher roughness of fracture surface in the epoxy droplet of hybrid fibers compared to bare ones suggests a more complex state of stress with considerable local variations of the direction of principal stresses along the fiber surface. The source of local stress variations can be the inhomogeneity of the matrix surrounding the hybrid fibers, due to reinforcing effect of nanofibers. The occurrence of this effect can also be inferred from the sub-micron diameter holes, observed in the SEM images of the epoxy coatings of pulled out hybrid fibers (Figure 13e). These holes are likely where individual nanofibers are pulled out of the epoxy during carbon fiber during junction failure. In other words, prior to nanofiber pull out, the nanofibers were carrying axial load and thus reinforcing the matrix. Therefore, because of reinforcing effect of nanofibers and mechanical interlocking between them and epoxy, the "weakest plane", where the junction failure is most likely, is pushed further away from the fiber, leading to cohesive failure. Hence, the fracture surface is expanded, demanding a larger force to initiate junction failure. The larger junction load capacity (~48%) manifests itself as increased IFSS (Figure 12). The above mentioned failure mechanism is schematically shown in Figure 14.

The proposed cohesive failure in epoxy-hybrid fiber junctions requires sufficiently strong bonding between PAN nanofibers and carbon fibers, without which a propagating interface crack could cause debonding between PAN and carbon fiber (adhesive failure) a scenario which was rarely observed (Figure 13b). The origin of this sufficiently strong bond, although expected to be primarily via physical bonds such as van der Waals forces,

is likely rooted in two causes: (i) the conformation of nanofibers to carbon fiber by vaporized surface tension between DMF and PAN as well as DMF and carbon fiber, and (ii) shrinkage of PAN nanofibers due to the combined plasticizing effect of the solvent vapor and heat which increases entropic forces within the fiber, as discussed in Section 2.

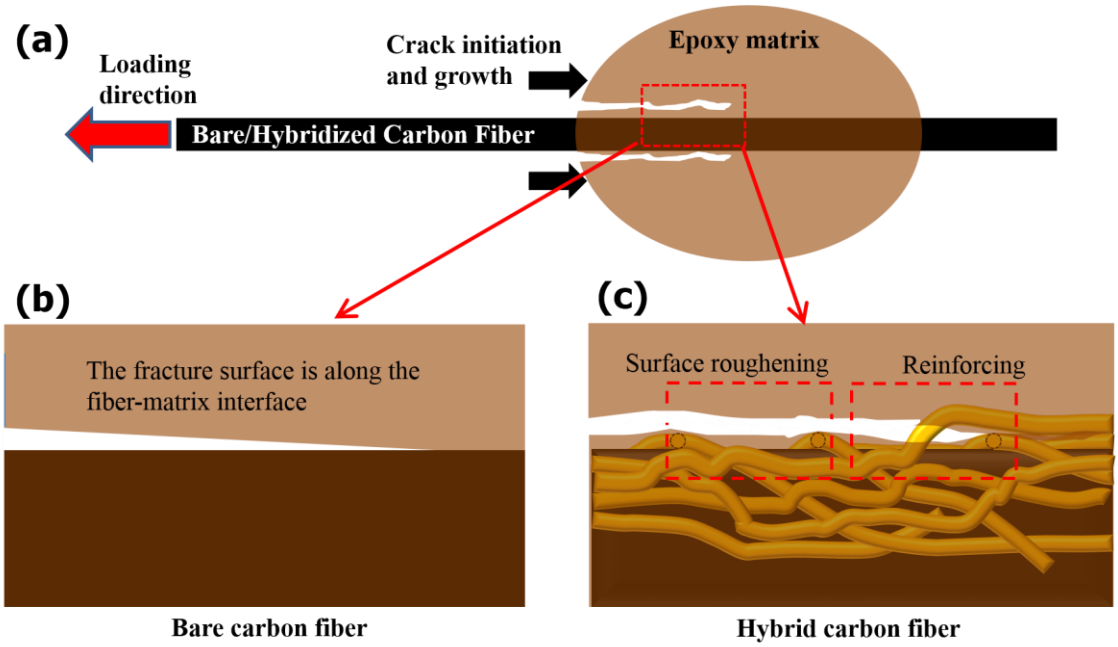

Figure 14. Schematics of fiber-epoxy junction failure mechanism: (a) a bare or hybridized carbon fiber embedded in epoxy micro-droplets. (b) Crack growth, leading to pull out, is dominantly along the bare fiber-epoxy interface, and mostly adhesive, as observed in SEM images of Figure 13. (c) In hybrid fibers, the junction failure is dominantly cohesive, with the junction crack being deflected away from fiber-epoxy interface, likely as a result of reinforcing effect of nanofibers and interlocking between nanofibers and matrix.

3.7. Conclusion

To evaluate the adhesion between carbon fiber and matrix, the two characterization, contact angle measurement and interfacial shear strength (IFSS) measurement, were

used. To measure contact angle, epoxy droplets were placed onto bare carbon fiber and hybridized carbon fiber by using a fine tip and then the contact angles were measured to compare the wettability of carbon fiber and hybridized carbon fiber. The result shows that the contact angle on hybridized carbon fiber is lower than that on bare carbon fiber, which indicates the better wettability of the hybridized carbon fiber. The increased wettability may be attributed to high rough surface as well as an affinity between nanofibers grafted on carbon fiber and epoxy matrix.

To measure the IFSS, the prepared carbon fiber and hybridized carbon fiber, where the epoxy microdroplets were placed, were pulled out from microdroplets by using a modified device. Pull-out test results shows that not only the interfacial shear strength of hybridized carbon fiber/epoxy microdroplets increased by ~48% compared to that of bare carbon fiber/epoxy microdroplets, but also the failure mode of the hybridized carbon fiber involved higher energy dissipation. In addition, postmortem SEM images were taken to observe the surface morphology of both carbon fiber and internal hole of microdroplet. The observation proves that hybridized carbon fiber can lead to cohesive failure by moving the failure plane away from carbon fiber surface to nanofiber-epoxy matrix interface. The failure of hybridized carbon fiber caused groove-like rough surface in the internal surface of droplets which means increased failure area that may lead to higher energy dissipation.

4. CONCLUSION AND FUTURE DIRECTIONS

4.1. Conclusion

The primary objective in this thesis was to enhance carbon fiber-matrix adhesion through developing a novel methodology which will overcome the challenges associated with the proposed methods, mainly surface functionalization of carbon fibers with functional groups which can form chemical and physical bonds with matrix and whiskerization of carbon fibers with nanofibers which can act as anchors inside matrix and increase the effective contact area between fiber and matrix.

In the functionalization, the fiber-matrix interface lies in 2 dimensions leading to a limited area to bear the applied load and dissipate mechanical energy, while the whiskerization can increase the load-bearing area via nanoparticles grown on the carbon fiber surface. The common whiskers are CNTs and CNFs which are bonded/grown on carbon fibers via a variety of methods, including CVD and electrophoresis. However, the whiskerization is commonly implemented at high temperature at least over 500℃ (CVD process) or in electrochemically corrosive environments (electrophoresis), thereby leading to thermal degradation of carbon fiber and decreased fiber strength.

To overcome the challenges, a new concept of hybrid carbon fiber was developed in this step through which polymeric nanofibers are deposited, with sufficient adhesion, on the surface of carbon fibers with no detectable damage to the carbon fiber, sizing or the

fiber itself. This novel whiskerization is through three steps, electrospinning process, solvent condensation, and stabilization. To demonstrate the feasibility of the method, PAN (polyacrylonitrile) nanofibers was grafted onto carbon fiber via electrospinning. Then, the adhesion between the PAN nanofibers and the carbon fiber was enhanced by exposing the nanofibers to the vapor of DMF solvent. Finally, the PAN nanofibers on the carbon fiber was thermally stabilization which will prevent the nanofibers from being dissolved in epoxy during epoxy curing process. Our studies led to the conclusion that the adhesion of nanofibers to carbon fibers was significantly enhanced via solvent vapor and thermal treatments through a combination of surface tension of DMF menisci condensed on the carbon fiber and the thermal activation of PAN chain mobility which led to shrinkage of nanofibers on carbon fibers, as a result of which nanofibers became tightly wrapped around carbon fiber.

We measured the affinity of carbon fibers to epoxy and its changes as a result of our whiskerization approach via epoxy-carbon fiber contact angle measurements and pull out experiments. The wettability studies, measuring contact angle of carbon fiber and epoxy microdroplets shows that the contact angle on hybridized carbon fiber is lower than that on bare carbon fiber, which indicates the better wettability of the hybridized carbon fiber. While the contact of the bare carbon fiber was 73.45°, that of the hybridized carbon fiber was 56.5°. The increased wettability may be attributed to high rough surface as well as an affinity between nanofibers grafted on carbon fiber and epoxy matrix. In other words, surface roughness can reduce the contact angle in surfaces

that are philic to each other. Pull-out test results shows that not only the interfacial shear strength of hybridized carbon fiber/epoxy microdroplets increased by ~48% compared to that of bare carbon fiber/epoxy microdroplets, but also the failure mode of the hybridized carbon fiber involved higher energy dissipation. In addition, Postmortem SEM images were taken to observe the surface morphology of both carbon fiber and internal hole of microdroplet. The observation proves that hybridized carbon fiber can lead to cohesive failure by moving the failure plane away from carbon fiber surface to nanofiber-epoxy matrix interface. Also, the nanofibers on the carbon fiber may act as reinforcements based on the evidence of many holes on the interface where cohesive failure occurs. The failure of hybridized carbon fiber caused groove-like rough surface in the internal surface of droplets which means increased failure area that may lead to higher energy dissipation.

4.2. Proposed Future Directions

In fiber reinforced composites, interlaminar cracks from within individual layers. The interlaminar cracking can give rise to separation of laminae in fiber reinforced composite, which is called delamination. When the interlaminar cracking faces carbon fiber, shear stress concentrates, thereby leading to debonding between carbon fiber and matrix. The delamination is substantially important in composites because it can reduce the role of strong fibers and finally can adversely affect the structural strength of composites.

To reduce the risk of delamination, the application of our method to carbon fiber mats is proposed for future direction. The proposed work is to deposit electrospun PAN nanofibers on carbon fiber mats, expose the nanofibers grafted on carbon fiber mats to the vapor of DMF solvent, and thermally stabilize them, similar to what was applied to individual nanofibers (Figure 15). Through this work, the nanofibers are expected to be well bonded onto carbon fiber via mechanisms such as surface tension of condensed solvent vapor and nanofiber thermal shrinkage, based on the results shown in the single hybridized carbon.

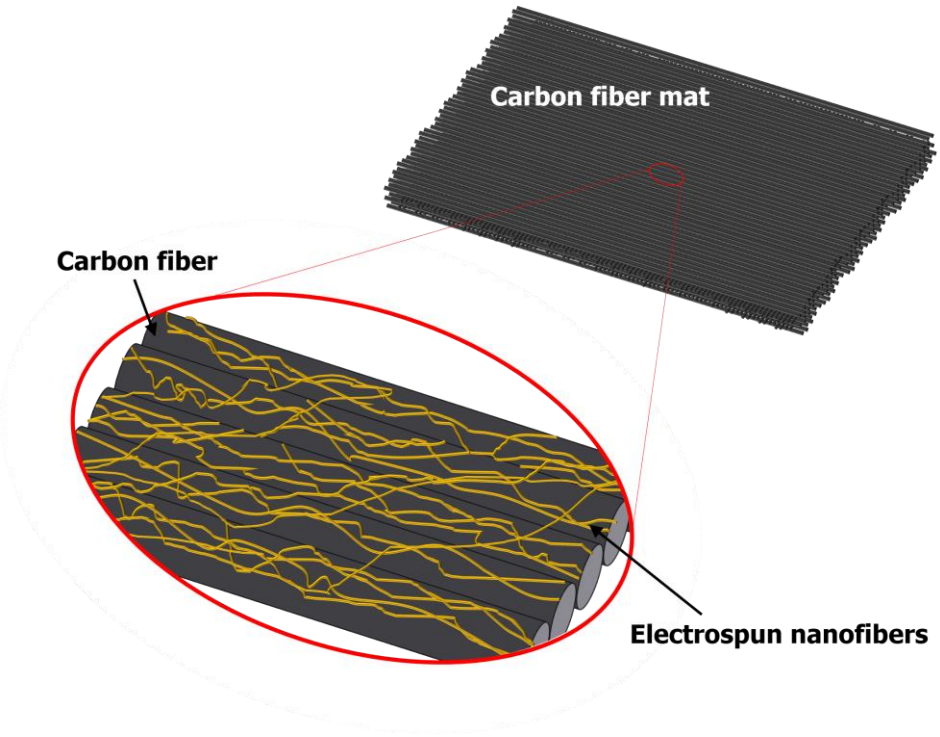

Figure 15. Schematic illustration of electrospun nanofibers deposited on carbon fiber.

The deposition of nanofibers onto carbon fiber mats may delay the delamination through moving the failure plane from carbon fiber-nanofiber interface to nanofiber-matrix interface. Ultimately, the change in failure plane will lead to cohesive failure with rough failure area indicating ductile behavior and high energy dissipation (Figure 16). This material processing should be followed up by mechanical characterization of the composites, including the double cantilever beam (DCB) test (mode I fracture toughness), the end notch flexure (ENF) test (pure mode II fracture toughness), and the edge crack torsion (ECT) test (pure mode III fracture toughness). A delamination may be loaded in those three modes, or a combination of the modes. Delamination and their growth are characterized by strain energy released rate (G).

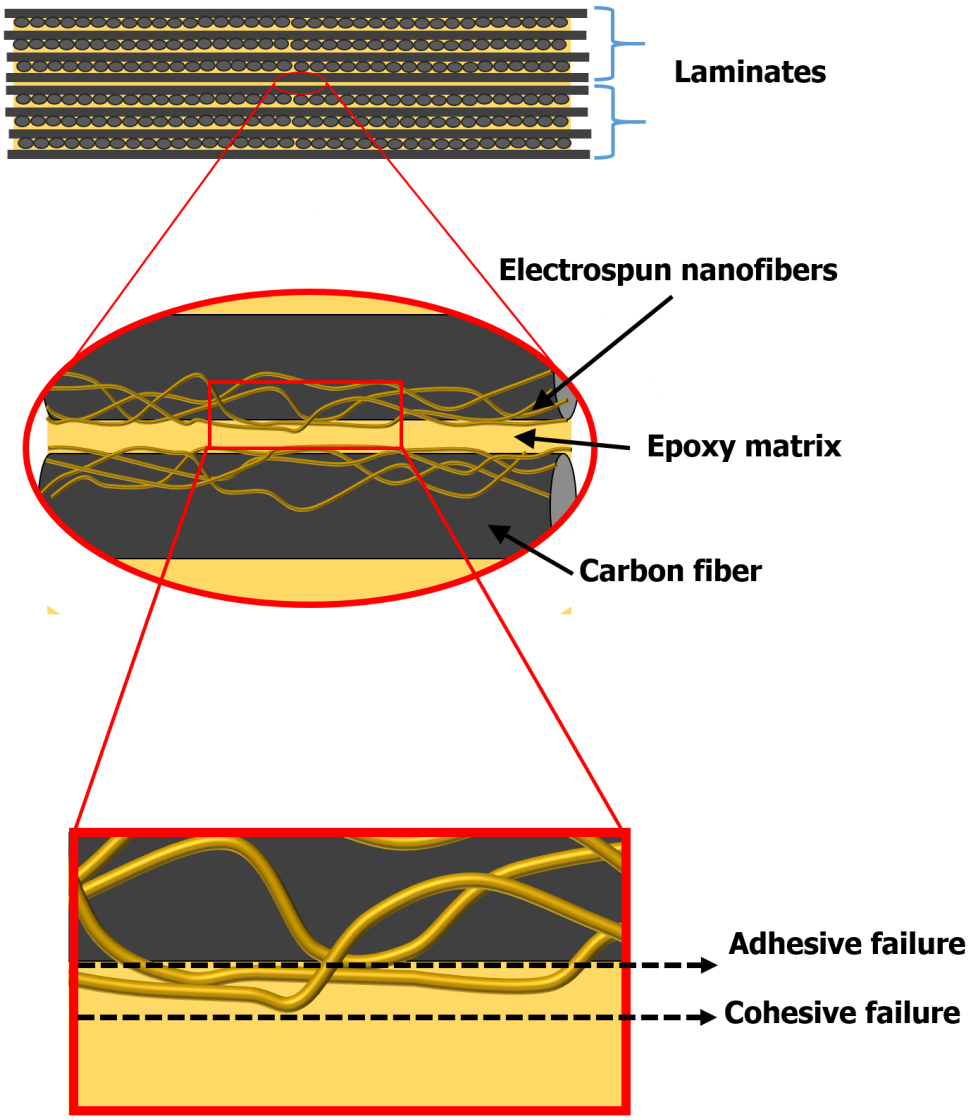

Figure 16. Schematic illustration of developed interface between laminates: the deposited nanofibers will change adhesive failure to cohesive as explained in Section 3.

REFERENCES

1. Donnet, J.-B., *Carbon fibers*. 1998: New York : Marcel Dekker, [1998] 3rd ed., rev. and expanded.
2. Park, S.-J., *Carbon Fibers*. Springer Series in Materials Science. 2014, Heidelberg: Springer.
3. Vajtai, R., *Springer handbook of nanomaterials*. 2013: Berlin : Springer, [2013].
4. Huang, X., *Fabrication and Properties of Carbon Fibers.* Materials, 2009. **2**(4): p. 2369.
5. Han, S. and D.D.L. Chung, *Increasing the through-thickness thermal conductivity of carbon fiber polymer–matrix composite by curing pressure increase and filler incorporation.* Composites Science and Technology, 2011. **71**(16): p. 1944-1952.
6. Newcomb, B.A., et al., *High resolution transmission electron microscopy study on polyacrylonitrile/carbon nanotube based carbon fibers and the effect of structure development on the thermal and electrical conductivities.* Carbon, 2015. **93**: p. 502-514.
7. Syayuthia R, s.u.e.m., et al., *Investigation of Flexure Strength on Carbon Fiber Reinforced Epoxy (CFRE) for Aircraft Panel.* Applied Mechanics & Materials, 2015. **786**: p. 79-83.

8. Wei-Li Wu, w.c. and q.c. Jiang-Kun Li, *Study on Carbon Fiber Reinforced Chloroprene Rubber Composites.* Advanced Materials Research, 2014(1052-1053): p. 254-257.

9. Lehmann, B.b.l.i.-d.d., et al., *Carbon Fiber Reinforced Composite - Toughness and structural integrity enhancement by integrating surface modified steel fibers.* Materials Science Forum, 2015. **825-826**: p. 425-432.

10. Liu, Y., et al., *An effective surface modification of carbon fiber for improving the interfacial adhesion of polypropylene composites.* Materials & Design, 2015. **88**: p. 810-819.

11. Yao, H., et al., *Optimization of interfacial microstructure and mechanical properties of carbon fiber/epoxy composites via carbon nanotube sizing.* Applied Surface Science, 2015. **347**: p. 583-590.

12. Madhukar, M.S. and L.T. Drzal, *Fiber-Matrix Adhesion and Its Effect on Composite Mechanical Properties: I. Inplane and Interlaminar Shear Behavior of Graphite/Epoxy Composites.* Journal of Composite Materials, 1991. **25**(8): p. 932-957.

13. Madhukar, M.S. and L.T. Drzal, *Fiber-Matrix Adhesion and Its Effect on Composite Mechanical Properties: II. Longitudinal (0°) and Transverse (90°) Tensile and Flexure Behavior of Graphite/Epoxy Composites.* Journal of Composite Materials, 1991. **25**(8): p. 958-991.

14. Madhukar, M.S. and L.T. Drzal, *Fiber-Matrix Adhesion and Its Effect on Composite Mechanical Properties. III. Longitudinal (0°) Compressive Properties*

of Graphite/Epoxy Composites. Journal of Composite Materials, 1992. **26**(3): p. 310-333.

15. Madhukar, M.S. and L.T. Drzal, *Fiber-Matrix Adhesion and Its Effect on Composite Mechanical Properties: IV. Mode I and Mode II Fracture Toughness of Graphite/Epoxy Composites.* Journal of Composite Materials, 1992. **26**(7): p. 936-968.
16. Totry, E., et al., *Effect of fiber, matrix and interface properties on the in-plane shear deformation of carbon-fiber reinforced composites.* Composites Science and Technology, 2010. **70**(6): p. 970-980.
17. Drzal, L.T., M. Madhukar, and M.C. Waterbury, *Adhesion to carbon fiber surfaces: Surface chemical and energetic effects.* Composite Structures, 1994. **27**(1–2): p. 65-71.
18. Macedo, F. and J.A. Ferreira, *Thermal contact resistance evaluation in polymer-based carbon fiber composites.* Review of Scientific Instruments, 2003. **74**(1): p. 828-830.
19. Krekel, G., K.J. Hüttinger, and W.P. Hoffman, *The relevance of the surface structure and surface chemistry of carbon fibres in their adhesion to high temperature thermoplastics.* Journal of Materials Science, 1994. **29**(13): p. 3461-3468.
20. Drzal, L.T., N. Sugiura, and D. Hook, *The role of chemical bonding and surface topography in adhesion between carbon fibers and epoxy matrices.* Composite Interfaces, 1996. **4**(5): p. 337-354.

21. Raghavendran, V.K., L.T. Drzal, and P. Askeland, *Effect of surface oxygen content and roughness on interfacial adhesion in carbon fiber–polycarbonate composites.* Journal of Adhesion Science and Technology, 2002. **16**(10): p. 1283-1306.

22. Li, J., *Interfacial studies on the ozone and air-oxidation-modified carbon fiber reinforced PEEK composites.* Surface and Interface Analysis, 2009. **41**(4): p. 310-315.

23. Kowbel, W., et al., *Effect of carbon fabric whiskerization on mechanical properties of C-C composites.* Composites Part A: Applied Science and Manufacturing, 1997. **28**(12): p. 993-1000.

24. Morgan, P., *Carbon Fibers and Their Composites*. 2005, Boca Raton: CRC Press.

25. Thostenson, E.T., C. Li, and T.-W. Chou, *Nanocomposites in context.* Composites Science and Technology, 2005. **65**(3–4): p. 491-516.

26. Chen, Q., et al., *Hybrid multi-scale epoxy composite made of conventional carbon fiber fabrics with interlaminar regions containing electrospun carbon nanofiber mats.* Composites Part A: Applied Science and Manufacturing, 2011. **42**(12): p. 2036-2042.

27. Qian, H., et al., *Carbon nanotube grafted carbon fibres: A study of wetting and fibre fragmentation.* Composites Part A: Applied Science and Manufacturing, 2010. **41**(9): p. 1107-1114.

28. Thostenson, E.T., et al., *Carbon nanotube/carbon fiber hybrid multiscale composites.* Journal of Applied Physics, 2002. **91**(9): p. 6034.

29. Sager, R.J., et al., *Effect of carbon nanotubes on the interfacial shear strength of T650 carbon fiber in an epoxy matrix.* Composites Science and Technology, 2009. **69**(7–8): p. 898-904.

30. Mathur, R.B., S. Chatterjee, and B.P. Singh, *Growth of carbon nanotubes on carbon fibre substrates to produce hybrid/phenolic composites with improved mechanical properties.* Composites Science and Technology, 2008. **68**(7–8): p. 1608-1615.

31. An, F., et al., *Preparation and characterization of carbon nanotube-hybridized carbon fiber to reinforce epoxy composite.* Materials & Design, 2012. **33**: p. 197-202.

32. De Greef, N., et al., *Growth of carbon nanotubes on carbon fibers without strength degradation.* Physica Status Solidi (B) Basic Research, 2012. **249**(12): p. 2420-2423.

33. Garcia, E.J., B.L. Wardle, and A. John Hart, *Joining prepreg composite interfaces with aligned carbon nanotubes.* Composites Part A: Applied Science and Manufacturing, 2008. **39**(6): p. 1065-1070.

34. Saba, J., et al., *Continuous electrodeposition of polypyrrole on carbon nanotube–carbon fiber hybrids as a protective treatment against nanotube dispersion.* Carbon, 2013. **51**: p. 20-26.

35. Li, W., et al., *Effect of carbon fiber surface treatment on Cu electrodeposition: The electrochemical behavior and the morphology of Cu deposits.* Journal of Alloys and Compounds, 2011. **509**(8): p. 3532-3536.

36. Schaefer, J.D., et al., *Effects of electrophoretically deposited carbon nanofibers on the interface of single carbon fibers embedded in epoxy matrix.* Carbon, 2011. **49**(8): p. 2750-2759.

37. Park, J.K., et al., *Electrodeposition of exfoliated graphite nanoplatelets onto carbon fibers and properties of their epoxy composites.* Composites Science and Technology, 2008. **68**(7–8): p. 1734-1741.

38. Zhang, J., et al., *Functional interphases with multi-walled carbon nanotubes in glass fibre/epoxy composites.* Carbon, 2010. **48**(8): p. 2273-2281.

39. Song, S., et al., *In situ study of copper electrodeposition on a single carbon fiber.* Journal of Electroanalytical Chemistry, 2013. **690**: p. 53-59.

40. Kuntz, M., et al., *Evaluation of interface parameters in push-out and pull-out tests.* Composites, 1994. **25**(7): p. 476-481.

41. Miller, B., P. Muri, and L. Rebenfeld, *A microbond method for determination of the shear strength of a fiber/resin interface.* Composites Science and Technology, 1987. **28**(1): p. 17-32.

42. Penn, L.S. and E.R. Bowler, *A new approach to surface energy characterization for adhesive performance prediction.* Surface and Interface Analysis, 1981. **3**(4): p. 161-164.

43. Ohsawa, T., et al., *Temperature dependence of critical fiber length for glass fiber-reinforced thermosetting resins.* Journal of Applied Polymer Science, 1978. **22**(11): p. 3203-3212.

44. Kelly, A. and W.R. Tyson, *Tensile properties of fibre-reinforced metals: Copper/tungsten and copper/molybdenum.* Journal of the Mechanics and Physics of Solids, 1965. **13**(6): p. 329-350.

45. Kolluru, P.V. and I. Chasiotis, *Interplay of molecular and specimen length scales in the large deformation mechanical behavior of polystyrene nanofibers.* Polymer, 2015. **56**: p. 507-515.

46. Naraghi, M. and S. Chawla, *Carbonized Micro- and Nanostructures: Can Downsizing Really Help?* Materials, 2014. **7**(5): p. 3820.

47. Naraghi, M., S.N. Arshad, and I. Chasiotis, *Molecular orientation and mechanical property size effects in electrospun polyacrylonitrile nanofibers.* Polymer, 2011. **52**(7): p. 1612-1618.

48. Behl, M. and A. Lendlein, *Shape-memory polymers.* Materials Today, 2007. **10**(4): p. 20-28.

49. Ya-Jen, Y., et al., *The effect of moisture absorption on the physical properties of polyurethane shape memory polymer foams.* Smart Materials and Structures, 2011. **20**(8): p. 085010.